

# B 13 How to Simulate Granular Matter

D. E. Wolf

Department of Physics

University Duisburg-Essen

## Contents

<b>1</b>	<b>What is granular matter and why do we simulate it?</b>	<b>2</b>
1.1	Not a liquid, not a solid . . . . .	2
1.2	Characterization at the grain level . . . . .	3
1.3	Bagnold scaling . . . . .	4
<b>2</b>	<b>Soft Particle Molecular Dynamics Simulations (MD)</b>	<b>4</b>
2.1	General Remarks . . . . .	4
2.2	Normal Force . . . . .	5
2.3	Tangential Force . . . . .	7
2.4	Detachment Effect and Brake Failure . . . . .	8
<b>3</b>	<b>Contact Dynamics Simulations (CD)</b>	<b>10</b>
3.1	General Remarks . . . . .	10
3.2	The single contact case . . . . .	11
3.3	Multi-contact systems . . . . .	14
<b>4</b>	<b>Comparison between CD and MD</b>	<b>15</b>
4.1	Computational effort . . . . .	15
4.2	Some recent applications . . . . .	17

# 1 What is granular matter and why do we simulate it?

## 1.1 Not a liquid, not a solid

Sand, pellets, coal, grains all have an important property: They can flow e.g. through hoppers, but in contrast to a fluid they also form piles. In fact compact granular matter can be hard like a solid: One needs not worry that ones child drowns in the sandbox. But under certain conditions the same granular matter can become dangerous: One can drown in a silo or in quicksand. This duality between fluid- and solid-like behaviour is the reason why granular matter has been of central technological importance since the beginnings of civilization: Solids can only be processed in the granular form.

Besides the technological importance and the exotic phenomena of granular matter, there are basic physical properties which make it an interesting research subject [1–3]. When it flows, it does so unlike an ordinary viscous fluid, but shows a nonlinear relationship between stress and strain-rate, and the separation of grains with different properties (e.g. large or small). When at rest, it does not behave like an ordinary elastic solid either, because of a nonlinear relation between stress and strain which depends on the fabric of the particle packing. Granular matter is not ergodic, its statistical physics is similar to the one of glass which freezes into metastable configurations. In particular the transition between flowing and static granular matter (“jamming”) poses many challenging and basic questions. Computer simulations are indispensable in order to trace these macroscopic phenomena back to the interactions between the particles.

With this goal in mind it becomes natural to restrict this lecture to discrete element methods (DEM). In a DEM all particle trajectories of a many particle system are calculated. Molecular Dynamics (MD) is the most versatile of these methods, but when applied to granular matter, it also has important limitations for rigid multi-contact systems and for rapid shear flows. In those cases Contact Dynamics (CD) avoids certain artefacts. Both simulation methods will be explained in the following for cohesionless spherical particles and contacts that do not exert torques (point contacts). Extensions are possible. They can be found e.g. in [1, 4] and in the new book by Pöschel and Schwager [5].

One speaks of granular matter, if one has a large number of particles (or grains) that can approximately be regarded as rigid bodies and interact weakly enough that they do not break up into fragments nor fuse into larger agglomerates. Any physical process that would change the particles is outside the primary scope of granular matter. Thus, the position of a particle is characterized by two vectors, its center of mass,  $\vec{r}$ , and a vector  $\vec{e}$  fixed inside the particle in order to describe its orientation in space. The equations of motion for a particle are

$$\frac{d}{dt}\vec{r} = \vec{v}, \quad m\frac{d}{dt}\vec{v} = \vec{F}, \quad (1)$$

$$\frac{d}{dt}\vec{e} = \vec{\omega} \times \vec{e}, \quad \frac{d}{dt}(\mathbf{I}\vec{\omega}) = \vec{T}. \quad (2)$$

$m$  and  $\mathbf{I}$  are the mass and the moment of inertia, respectively. Note that the tensor  $\mathbf{I}$  has to be calculated in the laboratory frame, where it in general depends on time, because its principal axes rotate together with the particle. Only for particles with spherical symmetry the moment of inertia is constant,  $\mathbf{I} = I\mathbf{1}$ . For simplicity, only this special case is considered in this lecture.  $\vec{v}$  and  $\vec{\omega}$  are the center of mass velocity, respectively the angular velocity.  $\vec{F}$  and  $\vec{T}$  denote the sum of all forces, respectively torques acting on the particle.

## 1.2 Characterization at the grain level

What is so special about the interactions between the particles compared to those between the molecules of a fluid or a solid, that granular matter deserves a separate lecture?

Although the enormous number of internal degrees of freedom of each individual particle is not taken into account explicitly, it gives rise to the first characteristic property of grain-grain interactions: They are irreversible, i.e. any relative motion of two grains in contact leads to energy dissipation. Examples are *solid friction* for tangential and *incomplete restitution* for normal relative motion. Solid friction is described by

$$\vec{\mathcal{R}}_t = -\mu_d \mathcal{R}_n \frac{\vec{\mathcal{V}}_t}{|\vec{\mathcal{V}}_t|}, \quad \text{for } \vec{\mathcal{V}}_t \neq 0, \quad (3)$$

where  $\mu_d$  is the coefficient of dynamic friction,  $\mathcal{R}_n$  the normal force, and  $\vec{\mathcal{V}}_t$  the relative tangential velocity of the two particles at the contact. It is important to distinguish the contact related quantities,  $\vec{\mathcal{R}}$  and  $\vec{\mathcal{V}}$ , from  $\vec{F}$ ,  $\vec{T}$ ,  $\vec{v}$ , and  $\vec{\omega}$  which are related to the center of mass of a particle. Incomplete restitution means that the ratio of the relative velocities after and before a binary head-on collision between spherical particles, the coefficient of restitution

$$e_n = |\mathcal{V}_n^{(f)} / \mathcal{V}_n^{(i)}|, \quad (4)$$

is smaller than 1. As a result of these dissipative interactions, relative motion of the particles gets damped out.

The second characteristic property of granular matter is that the grains must be big enough that their thermal energy  $k_B T$  can be neglected compared to their kinetic energy or to the potential energy barriers they encounter. For example, if one compares the gravitational energy difference on the length scale of the particle diameter with the thermal energy of room temperature under normal laboratory conditions, this requirement restricts the particle diameter to values larger than about  $1 \mu m$ . As a consequence, granular matter “freezes” into some metastable state under its own weight, as soon as one stops agitating it, e.g. by vibration or shearing.

A third characteristic property can most clearly be explained for perfectly rigid particles, which is the limit considered in Contact Dynamics simulations. The volume exclusion is a constraint that is only active if the distance between the particle surfaces (“gap”) is zero, and otherwise has no effect. The number of degrees of freedom in the system depends on the number of active constraints and is therefore itself a dynamical variable. The volume exclusion constraint implies that at every contact a repulsive constraint force  $\mathcal{R}_n$  is acting that can take whatever non-negative value is needed to prevent the interpenetration of the particles. This is expressed by the Signorini graph, on the left of Fig. 1.

A second type of constraint, the non-sliding constraint of frictional contacts, is only active, if the contact is closed and the tangential relative velocity  $|\vec{\mathcal{V}}_t|$  is zero. In this case the static friction force can be nonzero and assumes whatever tangential direction and value  $0 \leq |\vec{\mathcal{R}}_t| \leq \mu_s \mathcal{R}_n$  are needed to prevent sliding. This inequality means that the contact force  $\vec{\mathcal{R}} = (\mathcal{R}_n, \vec{\mathcal{R}}_t)$  for a sticking contact must lie inside a cone with opening angle  $\arctan(\mu_s)$  in force space, where  $\mu_s \geq \mu_d$  is the static friction coefficient. If a constraint force outside this Coulomb cone would be needed, sliding cannot be avoided, and one obtains the well defined sliding friction (3). The absolute values of the tangential velocity and the friction force lie on the Coulomb graph (right hand side of Fig. 1).

These constraints are switched on and off depending on the contact status (closed or open, sticking or sliding) and are an important source of nonlinear behaviour in granular matter.

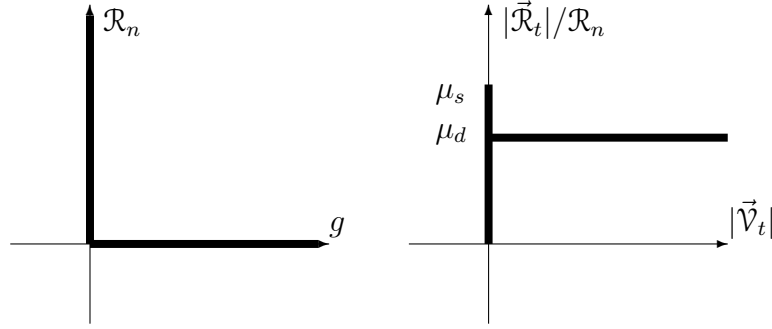


**Fig. 1:** Volume exclusion constraint (left): Allowed combinations of gap  $g$  and constraint force  $\mathcal{R}_n$  lie on the Signorini graph, i.e.  $g \geq 0$ ,  $\mathcal{R}_n \geq 0$ ,  $g \mathcal{R}_n = 0$ . Non-sliding constraint (right): The constraint force (static friction force) plus the sliding friction force constitute the Coulomb graph.

### 1.3 Bagnold scaling

The Signorini and the Coulomb graph have an important property: They are invariant under a rescaling of the forces  $\vec{\mathcal{R}} \rightarrow a\vec{\mathcal{R}}$ . If one simultaneously rescales the external forces by the same factor of  $a$ , time like  $t \rightarrow a^{-1/2}t$ , and accordingly the velocity and angular velocity like  $\vec{v} \rightarrow a^{1/2}\vec{v}$ ,  $\vec{\omega} \rightarrow a^{1/2}\vec{\omega}$ , then the equations of motion (1– 2) remain unchanged, because  $\vec{F}$  and  $\vec{M}$  are linear in the contact forces  $\vec{\mathcal{R}}$ . This very basic scaling property of granular matter is called “Bagnold scaling”. It means that granular matter flows only twice as quickly, if the driving forces are four times larger, in marked contrast to the linear response in ordinary liquids. This implies in particular that the confining pressure as well as the shear stress are proportional to the shear rate squared in granular matter:

$$\sigma_{xy} \propto (m/R)(\partial_y v_x)^2 \text{sign}(\partial_y v_x) \quad (5)$$

with a dimensionless proportionality constant.  $R$  denotes the radius of the particles. Bagnold [6] derived (5) by analyzing the momentum flux due to binary particle collisions, but the dimensional argument [7] shows that the scaling property is also valid in dense granular flows with lasting contacts [8, 9].

Many of the recent simulation studies concern the dependence of the proportionality constant in (5) on the various dimensionless parameters of the system [10], or the deviations from Bagnold scaling due to fixed force scales like gravity [11], finite elastic moduli [9] or adhesion forces [12, 13].

## 2 Soft Particle Molecular Dynamics Simulations (MD)

### 2.1 General Remarks

This chapter is based on more extended lecture notes [7] on simulations of granular matter. In molecular dynamics simulations Newton’s equations of motion (1– 2) are discretized and solved numerically to give the time evolution of a system of  $N$  particles. It should be borne in mind that this method like any DEM is based on a *model* of the contact forces, so that the results have a range of validity which needs to be assessed carefully.

In particular, in order to avoid the calculation of constraint forces, soft particle MD is designed such that the number of degrees of freedom is constant equal to three translations and three rotations per particle (in three dimensions). This requires that the volume exclusion and the non-sliding constraints have to be softened. The Signorini- and the Coulomb-graph are replaced by elastic force laws, which allow to calculate the contact forces as functions of the particle positions and velocities.

Within the soft particles model [14, 15] of granular matter one allows the particles to interpenetrate (“overlap”) somewhat. For spherical particles of radii  $R_i$  and  $R_j$  the overlap is

$$\xi_n = \max(0, R_i + R_j - |\vec{r}_i - \vec{r}_j|). \quad (6)$$

It is physically interpreted as a measure of the elastic deformation in normal direction at the contact. The overlap gives rise to a repulsive force which drives the particles apart. This will be discussed in the next section.

A simple, yet good scheme for integrating Newton’s equations of motion is the Leapfrog algorithm [16], which is briefly recalled here for later comparison with the integration scheme used in CD. Only the equations (1) will be considered here; the other two are treated correspondingly. Suppose one already knows  $\vec{v}(t - \Delta t/2)$ ,  $\vec{v}(t)$  and  $\vec{r}(t)$ . Then one proves by Taylor expansion that

$$\vec{v}\left(t + \frac{\Delta t}{2}\right) = \vec{v}\left(t - \frac{\Delta t}{2}\right) + \frac{1}{m} \vec{F}(t) \Delta t + O((\Delta t)^3) \quad (7)$$

$$\vec{v}(t + \Delta t) = \vec{v}\left(t + \frac{\Delta t}{2}\right) + \frac{1}{2m} \vec{F}(t) \Delta t + O((\Delta t)^2) \quad (8)$$

$$\vec{r}(t + \Delta t) = \vec{r}(t) + \vec{v}\left(t + \frac{\Delta t}{2}\right) \Delta t + O((\Delta t)^3) \quad (9)$$

Note that it suffices to determine  $\vec{v}(t + \Delta t)$ , which is needed for the force calculation of the next time step, only to second order in  $\Delta t$ , because the force is multiplied by  $\Delta t$ .

The discretization time step  $\Delta t$  should be about  $10^{-2}$  times the duration  $\tau$  of a binary collision in order to keep relative errors of physical quantities integrated over the whole collision time small of order  $10^{-4}$ . In contrast to Lennard-Jones fluids, where the characteristic time  $\tau \sim 10^{-13}$ sec, the collision time here is typically of the order  $\tau \sim 10^{-6}$ sec. The computational challenge of this method lies in the fact, that the hydrodynamic and the agitation time scales which one wants to investigate are vastly larger than the duration  $\tau$  of a binary collision.

## 2.2 Normal Force

A frequently used model for the normal component of the contact force is

$$\mathcal{R}_n = \max(0, \mathcal{R}_n^*) \quad (10)$$

with the test force [17]

$$\mathcal{R}_n^* = k\xi_n^\alpha + \gamma \frac{d}{dt} \xi_n^\alpha, \quad \alpha \geq 1, \quad (11)$$

which is identified with the normal component of the contact force, if it is positive. By convention, repulsive contact forces are counted as positive.

The term with coefficient  $k$  represents the elastic restoring force, and the one with coefficient  $\gamma$  is the result of viscous friction inside the particle. Whereas the first term is always non-negative, the second one is negative, when the overlap decreases: The internal friction acts together with the elastic restoring force to resist the approach of the centers of mass, but it effectively reduces the force with which the particles are driven apart. For small  $\xi$  the second term can even overcompensate the first one, when the particle centers are moving apart, so that the test force  $\mathcal{R}_n^*$  becomes negative. This would correspond to an attractive force, which is unphysical for non-cohesive particles. Due to the maximum condition in (10) the normal contact force is then set equal to zero. That the contact force vanishes, when there is still an overlap of the undistorted particle shapes, means that the elastically deformed particles separate before they have resumed their original form. The reason is that the centers of mass move apart faster than the viscoelastic bulk of the particles “flows” back into the undistorted form.

The exponent  $\alpha$  depends on the particle shape in the neighborhood of the contact. For spheres, Hertz derived the elastic part and showed that  $\alpha = 3/2$  [18]. Brilliantov et al. [19] derived the coefficients  $k$  and  $\gamma$  from linear viscoelasticity of the bulk of the particles. For disks (or parallel cylinders)  $\alpha = 1$ .

As explained in the previous section one needs to know a lower bound for the collision time  $\tau$  in order to choose the time step of the simulation appropriately. For this purpose the damping term in (10) can be neglected, because it can only increase the collision time. It is well known that in the linear case the collision time is given by

$$\tau = \sqrt{\frac{m_{\text{eff}}}{k}} \quad \text{for } \alpha = 1, \quad (12)$$

where  $m_{\text{eff}}$  is the reduced mass of the two collision partners. The case  $\alpha > 1$  can be viewed as a spring which becomes stiffer the more compressed it is. The effective stiffness can be estimated as

$$k_{\text{eff}} \approx k \xi_{\text{max}}^{\alpha-1}, \quad (13)$$

where the maximal overlap  $\xi_{\text{max}}$  can be related to the impact velocity by setting the elastic energy equal to the kinetic energy of the impact:

$$\frac{1}{\alpha+1} k \xi_{\text{max}}^{\alpha+1} = \frac{m_{\text{eff}}}{2} (\mathcal{V}_n^{(i)})^2 = E_{\text{kin}}^{(i)}. \quad (14)$$

As a result one obtains the estimate

$$\tau \approx \sqrt{\frac{m_{\text{eff}}}{k_{\text{eff}}}} \approx \left( \frac{m_{\text{eff}}}{k} \right)^{\frac{1}{1+\alpha}} (\mathcal{V}_n^{(i)})^{\frac{1-\alpha}{1+\alpha}}. \quad (15)$$

This shows that the time step has to be chosen according to the largest expected collision velocity, if  $\alpha > 1$ .

Similarly, using  $\xi_{\text{max}}$  as the characteristic length and  $\mathcal{V}_n^{(i)}$  as the characteristic velocity, one obtains a rough estimate of the damping term in (10):

$$\gamma \frac{d}{dt} \xi^\alpha \approx \gamma \xi_{\text{max}}^{\alpha-1} \mathcal{V}_n^{(i)}. \quad (16)$$

Integrating this damping force from  $\xi = 0$  to  $\xi = \xi_{\text{max}}$  and back gives another factor of  $\xi_{\text{max}}$  for the energy  $E_{\text{diss}}$  dissipated in a binary collision. For the coefficient of restitution  $e_n$  (4) this gives the following estimate:

$$1 - e_n^2 = \frac{E_{\text{diss}}}{E_{\text{kin}}^{(i)}} \approx \frac{\gamma}{m} \left( \frac{m}{k} \right)^{\frac{\alpha}{\alpha+1}} (\mathcal{V}_n^{(i)})^{\frac{\alpha-1}{\alpha+1}}. \quad (17)$$

Up to a numerical factor, this rough estimate gives the correct result for small velocities [7, 20]. It shows, that the coefficient of restitution for  $\alpha \neq 1$  depends on the collision velocity. In fact, experimentally one finds for a large class of materials [17, 21–23] that the restitution coefficient decreases with increasing  $\mathcal{V}_n$ , i.e. the more violent the impact, the more dissipative it is.

If the relative velocities do not vary over a wide range during a simulation, one often prefers to use the linear spring-dashpot model,  $\alpha = 1$ , where the restitution coefficient does not depend on the relative velocity. Together with the fact that the collision time does not depend on the velocity either, and that the linearity makes this law very well behaved numerically, the simple linear spring-dashpot model is a compromise between physical accuracy and numerical efficiency. Another reason for this is that it is tricky to implement a physically correct tangential force law consistent with  $\alpha = 3/2$  [24].

## 2.3 Tangential Force

In the previous section we have seen, how the excluded volume constraint is softened in MD simulations. In this section it will be shown, how the non-sliding constraint posed by static frictional contacts can be circumvented. The key observation is that a shear stress at a contact leads to a tangential elastic deformation of the particles. In a sticking contact the external shear stress can be compensated by the tangential elastic restoring force. However, if the shear stress exceeds a threshold, the contact breaks and the surfaces start to slide with respect to each other. The idea to implement tangential elasticity dates back to Cundall and Strack [14]. It has been improved by Brendel and Dippel [25] and further refined by Luding [15]. Here I present the implementation of Fazekas [26]. As soon as two particles touch, an imaginary spring is attached to the point of contact. Its displacement  $\vec{\xi}_t$  in the tangential plane represents the tangential elastic deformation of the particles (like the overlap  $\xi_n$  represents the normal elastic deformation). The calculation of  $\vec{\xi}_t$  is more subtle than the one of  $\xi_n$ , though, because its time derivative  $\frac{d}{dt}\vec{\xi}_t$  can only be identified with the tangential relative velocity at the contact,  $\vec{V}_t$ , if the contact is sticking. If it is sliding, the tangential elastic deformation is the microscopic origin of the sliding friction force (3), and  $\vec{\xi}_t$  must be calculated accordingly.

The tangential force is a function of  $\vec{\xi}_t$  and  $\vec{V}_t$ . First one uses a tangential linear spring-dashpot model with the tangential stiffness  $k_t$  and damping coefficient  $\gamma_t$  to calculate the test force

$$\vec{\mathcal{R}}_t^*(t) = -k_t \vec{\xi}_t(t) - \gamma_t \vec{V}_t(t). \quad (18)$$

If the contact has just been formed, the test force is  $\vec{\mathcal{R}}_t^*(t_0) = -\gamma_t \vec{V}_t(t_0)$ .

Then one checks, whether the absolute value of this test force is smaller than the static friction threshold. The formulas are particularly transparent, if the static and dynamic friction coefficient have the same value,  $\mu_s = \mu_d = \mu$ . If

$$|\vec{\mathcal{R}}_t^*(t)| \leq \mu \mathcal{R}_n(t), \quad (19)$$

the contact is regarded as sticking, and the test force is identified with the static friction force. If the threshold is exceeded, however, the contact is sliding, and one should use the dynamic friction (3). For the sake of computational efficiency, however, one simply rescales the absolute value of the test force keeping its direction fixed. In short, the tangential force is given by

$$\vec{\mathcal{R}}_t(t) = \frac{\vec{\mathcal{R}}_t^*(t)}{|\vec{\mathcal{R}}_t^*(t)|} \min \left( |\vec{\mathcal{R}}_t^*(t)|, \mu \mathcal{R}_n(t) \right). \quad (20)$$

Having determined all contact forces one can update the center of mass velocities and angular velocities of all particles. Hence one can calculate the relative velocities  $\vec{V}(t + \Delta t/2)$  at all contacts. This is needed for the update of the tangential spring.

In the sliding case the tangential elastic deformation should not increase. Moreover, the direction of the tangential force should then approach the one opposite to the tangential velocity. Therefore Fazekas [26] updates the tangential displacement by first calculating a test displacement

$$\vec{\xi}_t^*(t + \Delta t) = \vec{\xi}_t(t) + \vec{V}_t(t + \Delta t/2) \Delta t. \quad (21)$$

This is identified with the new tangential displacement, provided it does not give rise to an elastic restoring force of the tangential spring with an absolute value larger than  $\mu\mathcal{R}_n$ . In the latter case, the test displacement is rescaled maintaining its direction unchanged:

$$\vec{\xi}_t(t + \Delta t) = \frac{\vec{\xi}_t^*(t + \Delta t)}{|\vec{\xi}_t^*(t + \Delta t)|} \min \left( |\vec{\xi}_t^*(t + \Delta t)|, \frac{\mu\mathcal{R}_n(t + \Delta t)}{k_t} \right). \quad (22)$$

I have explained, how to calculate the tangential force for the special case that the normal vector does not change its direction. In the general case Luding [15] projects  $\vec{\xi}_t$  into the current tangential plane. In [26] a more complicated rotation into the current tangential plane is used.

## 2.4 Detachment Effect and Brake Failure

Eq.(15) shows that the collision time  $\tau$  and hence the simulation time step is proportional to  $k^{-1/(1+\alpha)}$ . As the phenomena one is interested in take place on much larger time scales, one common simulation strategy has been to choose  $k$  much smaller than in real materials, thereby allowing larger time steps. This seemed to be a good trade off for the artificially enlarged collision times. The restitution coefficient can be kept at a realistic value by choosing  $\gamma$  accordingly. Luding [27] showed that the artificial increase of  $\tau$  causes anomalously weak dissipation in dense systems, a simulation artefact called *detachment effect*. If the collision time is enlarged so much that it becomes comparable to the time between successive collisions (still much shorter than the times one is interested in) then the dynamical behaviour of the system changes drastically. Instead of having many successive binary collisions, one gets clusters of several particles overlapping at the same time.

Luding considers the simple example of a one dimensional equidistant arrangement of  $N$  grains, that move all with the same velocity  $v$  towards a wall, from which they are going to be reflected. If the distance is much smaller than  $v\tau$  then there is essentially a single multi-particle collision of all grains. The whole cluster can be viewed as a single elastic particle with a total deformation  $N\xi_{max}$ . The collision time of the cluster is then  $N$  times the collision time of a binary collision. For the linear spring-dashpot model this implies that the dissipated energy per particle is the same as in a single binary collision. By contrast, if the distance between the particles initially was much larger than  $v\tau$  then one gets a sequence of about  $N^2/2$  binary collisions until all particles are reflected. The dissipated energy per particle is significantly increased. This example shows that dissipation is suppressed in dense systems, if one artificially increases  $\tau$  in order to be able to simulate larger time intervals.

Soft particle molecular dynamics gives also rise to another artefact, the so-called *brake failure effect* [28]. Consider two equal spheres of radius  $R$  that collide with initial relative velocity  $\vec{V}^{(i)}$  under an angle  $\vartheta$  (Fig.2). We choose cartesian coordinates such that  $\vec{V}^{(i)}$  points in  $x$ -direction.



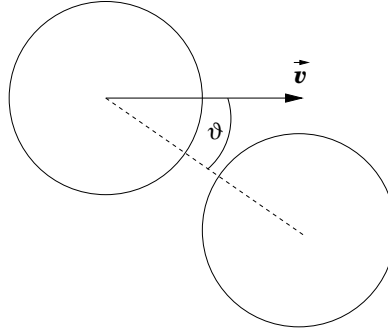


**Fig. 2:** Two spheres colliding under an angle  $\vartheta$ . In soft particle MD they may penetrate each other without being properly reflected (brake-failure artefact).

A braking function can be defined as the change of  $\mathcal{V}_x$  caused by the interaction between the colliding spheres,

$$\Delta \mathcal{V}_x \propto \int_{t_\xi} \mathcal{R}_x(t) dt, \quad (23)$$

where  $t_\xi$  is the time for which the spheres overlap. If they could freely penetrate each other without feeling any interaction, they would overlap for a time

$$\tau_0 = 4R \cos \vartheta / |\vec{\mathcal{V}}^{(i)}|. \quad (24)$$

As long as  $\tau \ll \tau_0$ , the simulation gives correct results: The contact time is determined by the collision time (15),  $t_\xi \approx \tau$ . Then the spheres are reflected from each other, i.e.

$$\Delta \mathcal{V}_x \propto |\vec{\mathcal{V}}^{(i)}| \quad (25)$$

with geometrical factors depending on  $\vartheta$ . The braking function increases linearly with the initial velocity.

However, for  $\tau_0 \ll \tau$ , the braking function behaves unphysically. The contact exists only for a short time  $t_\xi \approx \tau_0$ . The integral (23) can be approximated by  $\int \mathcal{R}_x(t) dt \approx \bar{\mathcal{R}}_x \tau_0$ , where  $\bar{\mathcal{R}}_x$  is a mean force in  $x$ -direction. Using (24) we obtain:  $\Delta \mathcal{V}_x \propto 1/|\vec{\mathcal{V}}^{(i)}|$ . This decrease of the braking function with increasing initial velocity is meant by the term *brake failure*.

The transition between both regimes takes place at  $\tau_0/\tau \approx 1$ , so that we obtain a critical velocity for brake failure,

$$\mathcal{V}_c = \frac{4R \cos \vartheta}{\tau}. \quad (26)$$

MD simulations of particle collisions exhibit an unrealistically small dissipation when the impact velocity exceeds the critical velocity  $\mathcal{V}_c$ . This artefact occurs e.g. for rapid shear flows [28]. It should be emphasized that it cannot be cured by choosing a smaller time step: The brake failure phenomenon has its origin in the penetrability of the particles, not in the discretization of time.

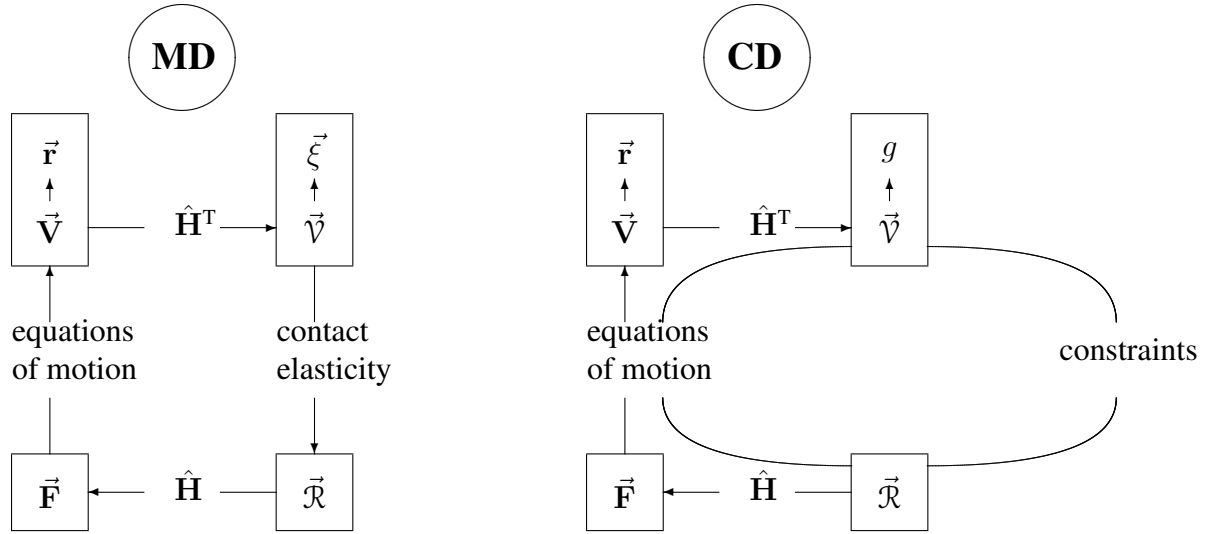


**Fig. 3:** A time step in MD is the cycle starting with the particle positions and velocities, from which one obtains the elastic contact displacement  $\vec{\xi}$  and relative velocities  $\vec{V}$ . These determine the contact forces  $\vec{R}$ , from which one calculates the forces and torques  $\vec{F}$  needed for the equations of motion. In CD all relative velocities and contact forces are determined together by making the time step of the equations of motion consistent with the constraints. The matrices  $\hat{H}$  and  $\hat{H}^T$  are explained in the text.

### 3 Contact Dynamics Simulations (CD)

#### 3.1 General Remarks

This chapter is an excerpt of a recent introduction of the method for beginners [29], where also further details and references can be found. The method is rather new [30].

Contact Dynamics is a discrete element method like Molecular Dynamics. However, it can handle rigid particles and static frictional contacts without regularizing the graphs, Fig. 1. Hence it is able to overcome some difficulties that arise in soft particle molecular dynamics. On the other hand, by considering the particles as perfectly rigid, contact dynamics suppresses phenomena caused by particle deformation. It represents the deformation of the granular medium as a whole in an idealized way exclusively by particle rearrangements.

Imposing constraints requires implicit forces (constraint forces) which cannot be calculated from the positions and velocities of the particles alone. The constraint forces are determined such as to compensate all forces that would cause constraint-violating accelerations (see Fig.3). Collisions of rigid particles give rise to discontinuous velocities during the time-evolution. In such non-smooth mechanics [31,32] the use of second or higher order schemes for the numerical integration of the motion is not beneficial and could even be problematic. Therefore an implicit Euler integration is applied in our CD code:

$$\vec{v}(t + \Delta t) = \vec{v}(t) + \frac{1}{m} \vec{F}(t + \Delta t) \Delta t + O((\Delta t)^2). \quad (27)$$

$$\vec{r}(t + \Delta t) = \vec{r}(t) + \vec{v}(t + \Delta t) \Delta t + O((\Delta t)^2). \quad (28)$$

The forces  $\vec{F}$  are calculated in each step such that the constraints remain fulfilled.

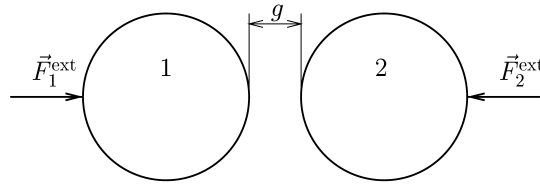


**Fig. 4:** Two rigid particles with an incipient contact. A contact force  $\vec{\mathcal{R}}$  appears in a time step, in which the gap  $g$  is closing (or, when it was already closed, if it is not opening).

### 3.2 The single contact case

We consider a pair of rigid spheres already in contact or with a small gap between them. They are numbered 1 and 2 and are subject to constant external forces  $\vec{F}_1^{\text{ext}}, \vec{F}_2^{\text{ext}}$  acting on the centers of mass (Fig. 4). It is useful to introduce generalized velocity and force vectors:

$$\vec{\mathbf{V}} = \begin{bmatrix} \vec{v}_1 \\ \vec{\omega}_1 \\ \vec{v}_2 \\ \vec{\omega}_2 \end{bmatrix}, \quad \vec{\mathbf{F}} = \begin{bmatrix} \vec{F}_1 \\ \vec{T}_1 \\ \vec{F}_2 \\ \vec{T}_2 \end{bmatrix}, \quad \vec{\mathbf{F}}^{\text{ext}} = \begin{bmatrix} \vec{F}_1^{\text{ext}} \\ \vec{0} \\ \vec{F}_2^{\text{ext}} \\ \vec{0} \end{bmatrix}, \quad (29)$$

where  $\vec{\mathbf{F}}$  contains the interaction forces and torques, while  $\vec{\mathbf{F}}^{\text{ext}}$  contains the external forces (external torques are not taken into account here).

Volume exclusion and Coulomb friction may require a constraint force  $\vec{\mathcal{R}}$ , where we use the convention that  $\vec{\mathcal{R}}$  acts on particle 2 while its reaction force  $-\vec{\mathcal{R}}$  acts on particle 1. The constraint force  $\vec{\mathcal{R}}$  enters the equations of motion for the particle degrees of freedom in terms of interaction forces  $\vec{F}_i$  and interaction torques  $\vec{T}_i$ ,

$$\vec{F}_1 = -\vec{\mathcal{R}}, \quad \vec{F}_2 = \vec{\mathcal{R}}, \quad \vec{T}_1 = -\vec{l}_1 \times \vec{\mathcal{R}}, \quad \vec{T}_2 = \vec{l}_2 \times \vec{\mathcal{R}}, \quad (30)$$

where the vectors  $\vec{l}_1$  and  $\vec{l}_2$  point from the centers of mass to the expected contact point. According to (30), the generalized force vector  $\vec{\mathbf{F}}$  is a linear transformation of  $\vec{\mathcal{R}}$ ,

$$\vec{\mathbf{F}} = \hat{\mathbf{H}} \vec{\mathcal{R}}. \quad (31)$$

The relative velocity at the contact,

$$\vec{\mathcal{V}} = \vec{v}_2 + \vec{\omega}_2 \times \vec{l}_2 - (\vec{v}_1 + \vec{\omega}_1 \times \vec{l}_1), \quad (32)$$

is also linearly related to the generalized velocity vector:

$$\vec{\mathcal{V}} = \hat{\mathbf{H}}^T \vec{\mathbf{V}}, \quad (33)$$

where  $\hat{\mathbf{H}}^T$  is the transpose of the matrix  $\hat{\mathbf{H}}$ . These two matrices describe the geometry and allow to transform contact quantities into particle quantities and vice versa (see Fig.3). They are in general not quadratic (in the present example  $\hat{\mathbf{H}}$  is a  $12 \times 3$  matrix).

The equations of motion for the two particles read:

$$\frac{d\vec{\mathbf{V}}}{dt} = \hat{\mathbf{M}}^{-1}(\vec{\mathbf{F}} + \vec{\mathbf{F}}^{\text{ext}}), \quad \hat{\mathbf{M}} = \begin{bmatrix} m_1 \mathbf{1} & 0 & 0 & 0 \\ 0 & I_1 \mathbf{1} & 0 & 0 \\ 0 & 0 & m_2 \mathbf{1} & 0 \\ 0 & 0 & 0 & I_2 \mathbf{1} \end{bmatrix}. \quad (34)$$

$\hat{\mathbf{M}}^{-1}$  is the inverse of the generalized  $12 \times 12$  mass matrix  $\hat{\mathbf{M}}$ , which contains the masses and moments of inertia of the particles ( $\mathbf{1}$  denotes the  $3 \times 3$  unit matrix).

In order to determine the constraint force  $\vec{\mathcal{R}}$ , one transforms Eq. (34) into an equation for the relative velocity  $\vec{\mathcal{V}}$  by applying  $\hat{\mathbf{H}}^T$  (note that a term  $(d\hat{\mathbf{H}}^T/dt) \mathbf{V}$  describing the geometrical change is neglected here, which is typically a good approximation) :

$$\frac{d\vec{\mathcal{V}}}{dt} = \hat{\mathcal{M}}^{-1} \vec{\mathcal{R}} + \frac{d\vec{\mathcal{V}}^{\text{free}}}{dt} , \quad (35)$$

$$\text{with } \frac{d\vec{\mathcal{V}}^{\text{free}}}{dt} = \hat{\mathbf{H}}^T \hat{\mathbf{M}}^{-1} \vec{\mathbf{F}}^{\text{ext}} , \quad \text{and } \hat{\mathcal{M}}^{-1} = \hat{\mathbf{H}}^T \hat{\mathbf{M}}^{-1} \hat{\mathbf{H}} . \quad (36)$$

$d\vec{\mathcal{V}}^{\text{free}}/dt$  has the meaning of the acceleration without any interaction between the particles, and  $\hat{\mathcal{M}}$  denotes the reduced mass matrix of the contact.  $\hat{\mathcal{M}}^{-1}$  has a simple form in the case of spheres:

$$\hat{\mathcal{M}}^{-1} = \frac{1}{m_n} \vec{n} \otimes \vec{n} + \frac{1}{m_t} (\mathbf{1} - \vec{n} \otimes \vec{n}) , \quad (37)$$

$$\frac{1}{m_n} = \frac{1}{m_1} + \frac{1}{m_2} , \quad \frac{1}{m_t} = \frac{1}{m_n} + \frac{\vec{l}_1^2}{I_1} + \frac{\vec{l}_2^2}{I_2} . \quad (38)$$

Here  $\vec{n}$  denotes the unit vector perpendicular to the tangent plane, pointing from particle 1 towards particle 2. The tensorial product  $\vec{n} \otimes \vec{n}$  is the  $3 \times 3$  matrix with elements  $n_\mu n_\nu$ . Eq. (37) shows that normal and tangential components are not coupled for spheres.

Solving Eq.(35) for the contact force in the Euler-scheme (27) one obtains

$$\vec{\mathcal{R}}^{\text{new}} = \hat{\mathcal{M}} \frac{\vec{\mathcal{V}}^{\text{new}} - \vec{\mathcal{V}}^{\text{free,new}}}{\Delta t} , \quad (39)$$

where according to Eq.(36)

$$\vec{\mathcal{V}}^{\text{free,new}} = \vec{\mathcal{V}} + \hat{\mathbf{H}}^T \hat{\mathbf{M}}^{-1} \vec{\mathbf{F}}^{\text{ext}} \Delta t \quad (40)$$

has the meaning of the new velocity if there was no interaction. Here and in the following the superscript “new” refers to the value at time  $t + \Delta t$ , while values of  $g$ ,  $\vec{\mathcal{V}}$  and  $\vec{\mathcal{R}}$  without this superscript are taken at time  $t$ .

In order to determine the two unknowns, the contact force  $\vec{\mathcal{R}}^{\text{new}}$  and the relative velocity  $\vec{\mathcal{V}}^{\text{new}}$ , one has to combine the linear relation (39) with the volume exclusion and non-sliding constraints. This is done in three steps in the algorithm.

1. First we check whether the gap  $g$  remains positive after the time step  $\Delta t$ , if the interaction between the particles is not taken into account, i.e. whether

$$g + \mathcal{V}_n^{\text{free,new}} \Delta t > 0 . \quad (41)$$

If condition (41) is fulfilled the incipient contact did not close during the time step so that the contact force is zero,  $\vec{\mathcal{R}}^{\text{new}} = 0$ , and  $\vec{\mathcal{V}}^{\text{new}} = \vec{\mathcal{V}}^{\text{free,new}}$ . If the left hand side of Eq. (41) is zero or negative, the algorithm continues with the second step.

2. In this step the algorithm makes an attempt to establish a non-sliding contact, i.e. we require that the gap closes *and* that no slip occurs:

$$g + \mathcal{V}_n^{\text{new}} \Delta t = 0 , \quad \vec{\mathcal{V}}_t^{\text{new}} = 0 . \quad (42)$$

Therefore the new velocity is  $\vec{V}^{\text{new}} = -(g/\Delta t)\vec{n}$ . This determines the contact force Eq.(39):

$$\vec{\mathcal{R}}^{\text{new}} = -\frac{1}{\Delta t}\hat{\mathcal{M}}\left(\frac{g}{\Delta t}\vec{n} + \vec{V}^{\text{free,new}}\right). \quad (43)$$

However, this contact force can only be accepted if it lies within the Coulomb cone  $|\vec{\mathcal{R}}_t| \leq \mu\mathcal{R}_n$ . If this does not hold, we have to give up the assumption of a non-sliding contact. Then the contact will be a sliding one and  $\vec{\mathcal{R}}^{\text{new}}$  is recalculated in the third step.

3. For a sliding contact the first condition (42) remains valid, but the second one not. Then  $\vec{V}_t^{\text{new}}$  must be determined together with  $\vec{\mathcal{R}}_t^{\text{new}}$  from the following condition: The tangential part of

$$\vec{\mathcal{R}}^{\text{new}} = -\frac{1}{\Delta t}\hat{\mathcal{M}}\left(\frac{g}{\Delta t}\vec{n} - \vec{V}_t^{\text{new}} + \vec{V}^{\text{free,new}}\right) \quad (44)$$

must be equal to sliding friction, i.e.

$$\vec{\mathcal{R}}_t^{\text{new}} = -\mu\mathcal{R}_n^{\text{new}} \frac{\vec{V}_t^{\text{new}}}{|\vec{V}_t^{\text{new}}|}. \quad (45)$$

There are only three unknowns, the normal component of  $\vec{\mathcal{R}}^{\text{new}}$  and the tangential components of  $\vec{V}^{\text{new}}$ . The three equations (44) (one for each component) determine these unknowns.

These three points form a *contact law* that in general provides the contact force in every time step. It can be applied for colliding particles, but also for pre-existing contacts. In this respect no distinction has to be made.

Eq.(42) implies that after the collision of the two spheres the gap is zero. The particles do not bounce back: Their coefficient of restitution is zero. How nonzero restitution coefficients can be implemented is described in [32]. In dense granular media it is justified to work with a coefficient of restitution of zero, though: As they provide an enormous amount of collective dissipation mechanisms due to rearrangements, frustrated rotations etc. a grain hitting such a packing will hardly bounce back: The effective restitution coefficient is close to zero.

Due to practical reasons a slight change is recommended in the contact law [31], namely the application of  $g^{\text{pos}} = \max(g, 0)$  instead of  $g$  in Eqs. (43) and (44). This, in principle, makes no difference because  $g$  should be non-negative. However, due to inaccurate calculations some small overlaps can be created between neighboring particles. These overlaps would be immediately eliminated in the first version of the inelastic contact law by applying a larger repulsive force in order to satisfy the first equation (42). This self-correcting mechanism, however, has the drawback that it pumps kinetic energy into the system, when thrusting the overlapping particles away from each other. With the application of  $g^{\text{pos}}$  one avoids this. Moreover an already existing overlap is not eliminated, only its further growth is inhibited. This can be used to monitor the numerical inaccuracies of a CD-simulation.

Simulations may involve also certain confining objects (e.g. container, fixed wall, moving piston, rotating drum). Therefore the algorithm has to be able to handle not only sphere-sphere contacts, but also sphere-plane and sphere-cylinder contacts. One can easily verify that the same simple contact law can be applied as the one derived here for spheres, if planes and cylinders with infinite moments of inertia are used ( $I_2 = \infty$ ).

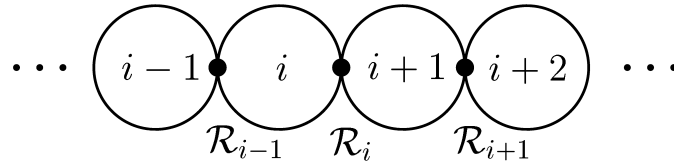


**Fig. 5:** A one dimensional array of spheres in contact.

### 3.3 Multi-contact systems

So far we have only discussed how to treat a single incipient or existing contact in the framework of Contact Dynamics. However, the most interesting applications of CD involve dense granular media where many particles interact simultaneously within a contact network that may span a substantial part of the whole system.

A simple one-dimensional example is given in Fig. 5. Let us assume, that none of the contacts has freshly formed in the last time step, so that all gaps  $g_i$  and all relative velocities  $\mathcal{V}_i$  are zero, but that the whole array will be accelerated or perhaps disrupted by some external forces acting only on some far away particles of the chain which are not depicted in Fig. 5. Eq.(43) can be used for the calculation of the constraint force at the  $i$ -th contact, but the role of the external forces is now played by the constraint forces of the neighboring contacts. Replacing  $\vec{F}_2^{\text{ext}}$  by  $-\vec{\mathcal{R}}_{i+1}^{\text{new}}$  and  $\vec{F}_1^{\text{ext}}$  by  $\vec{\mathcal{R}}_{i-1}^{\text{new}}$  in Eq.(40) one obtains

$$\mathcal{R}_i^{\text{new}} = \frac{1}{2} (\mathcal{R}_{i-1}^{\text{new}} + \mathcal{R}_{i+1}^{\text{new}}), \quad (46)$$

where we used that the reduced mass is  $\mathcal{M} = m/2$  in this simple case. This is a discretized Laplace equation which couples all constraint forces in the contact network. When replacing  $\vec{F}_i^{\text{ext}}$  by the contact forces from neighboring particles in three dimensions, one should not forget that they exert also torques  $\vec{T}_1^{\text{ext}}$  and  $\vec{T}_2^{\text{ext}}$ . They have to be included in the generalized vector  $\mathbf{F}^{\text{ext}}$  in Eq.(29), where the two torques originally were set to zero.

The example Fig. 5 shows that using constraint forces has an important consequence: A contact force depends also on adjacent contact forces that press the two particles together. Thus for a compressed cluster of rigid particles the contact forces cannot be computed locally. Whereas in the simple one-dimensional example of Eq.(46) the exact calculation of globally consistent constraint forces is feasible, it becomes exceedingly cumbersome for large, complex three-dimensional contact networks. There may even be more than one solution satisfying all constraints [33,34]. Different algorithms have been used to determine globally consistent constraint forces (e.g. [33,35]), but in general one uses an iterative scheme (called the *iterative solver*). It is applied in every time step before the implicit Euler integration can proceed one step further with the newly provided forces.

This method works as follows. At each iteration step we update every existing or incipient contact independently in the sense that a “new” contact force is calculated based on the contact law for the one-contact case, presuming that the current forces of the neighboring contacts were already the correct ones. The resulting force is stored for the given contact and a new contact is chosen for the next update. In that way all the contact forces are updated one by one sequentially. Of course, one update per contact (i.e. one iteration step) does not yet provide a global

solution. Such iteration steps have to be repeated many times letting the forces relax according to their neighborhood towards a globally consistent state. After satisfactory convergence is reached the iteration loop can be stopped. With convergence we mean that a further update of the contact forces gives only negligible changes, thus the constraint conditions are practically fulfilled for the whole system. The applied number of iterations  $N_I$  within one time step depends on the accuracy of the convergence criterion [36, 37]. Higher  $N_I$  provide more accurate forces but require larger computation time.

As an example let us return to the one-dimensional example, Eq.(46). If one associates a virtual time step  $\Delta t^* = \Delta t/N_I$  with each of the  $N_I$  iteration steps performed within a single real time step  $\Delta t$  of the simulation, the forces relax towards a consistent solution of the equations (46) according to

$$\frac{\mathcal{R}_i(t^* + \Delta t^*) - \mathcal{R}_i(t^*)}{\Delta t^*} = \frac{N_I}{2\Delta t} (\mathcal{R}_{i+1}(t^*) - 2\mathcal{R}_i(t^*) + \mathcal{R}_{i-1}(t^*)), \quad (47)$$

i.e. the change of  $\mathcal{R}_i$  per iteration step is equal to the difference between the left and right hand side of the consistency equation (46). The virtual time evolution (47) is simply a discretized one-dimensional diffusion equation [38] with diffusion constant

$$D \propto N_I \frac{R^2}{\Delta t}. \quad (48)$$

Also in three dimensions, the force consistency with the constraints spreads diffusively during the iteration. For a system of linear size  $L$  convergence requires  $D\Delta t > L^2 \sim (N^{1/d}R)^2$ , where  $N$  is the number of particles in the system, which is assumed to be connected throughout, and  $d$  is the space dimension. This implies

$$N_I > N^{2/d}. \quad (49)$$

The number of iterations needed to reach convergence of the constraint forces for a single time step grows with the number of particles in the system.

Regarding the order of the update sequence within the list of (existing and incipient) contacts, it is preferably random and different for each sweep. In this way one avoids any bias in the information spreading. It has to be mentioned that the *random sweep* described here differs from the well known *random sequential update*: While in the latter the choice of a contact is independent of the previous choices (the same contact could be selected twice), the *random sweep* selects each contact exactly once within one iteration step. We note that in contrast to this sequential process, a simple parallel update would be unstable.

## 4 Comparison between CD and MD

(Based on [29].) The Contact Dynamics algorithm has been applied to investigate the physics of dense granular media by more and more scientists over the last decade, but still Molecular Dynamics is much wider known and often regarded as easier. This does not mean that Contact Dynamics is less powerful. On the contrary, The two techniques have complementary strengths.

### 4.1 Computational effort

In this section we estimate the computing time  $T_{\text{comp}}$  needed for the simulation of a dense  $N$ -particle system in  $d$  dimensions for a certain real time  $T_{\text{real}}$ . This gives a certain guidance, for what problems it is advantageous to use Contact Dynamics instead of Molecular Dynamics.

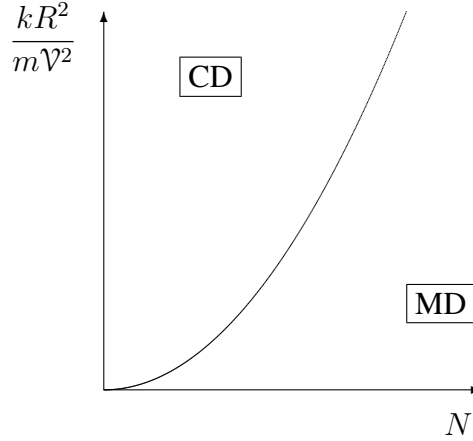


**Fig. 6:** Domains where CD, respectively MD simulations are more efficient are separated by a power law  $N^{4/d}$ .

In the derivation of the contact law changes of the matrix  $\hat{\mathbf{H}}$  were neglected. This is only justified if the relative displacement of adjacent particles during one time step is small compared to the particle size and to the radius of curvature of the surfaces in contact. This means that the time step in contact dynamics must be a fraction of  $R/\mathcal{V}$ , where  $\mathcal{V}$  is a typical relative velocity and  $R$  a typical radius of curvature. Each time step requires  $N_I \sim N^{2/d}$  force iterations, each of which takes order  $N$  computations. Hence the computational effort for a Contact Dynamics simulation is

$$T_{\text{comp}}^{(\text{CD})} \sim N^{1+2/d} T_{\text{real}} \mathcal{V}/R. \quad (50)$$

In molecular dynamics with elastic interactions modelled by a linear spring of stiffness  $k$  each collision must be time resolved, so that a much shorter time step than in CD is needed. It must be a fraction of the duration of a collision,  $\sqrt{m/k}$ , where  $m$  is the particle mass. The computational effort per time step, however, scales only with the particle number  $N$ . Hence

$$T_{\text{comp}}^{(\text{MD})} \sim N T_{\text{real}} \sqrt{k/m}. \quad (51)$$

Putting this together we conclude that

$$\frac{T_{\text{comp}}^{(\text{CD})}}{T_{\text{comp}}^{(\text{MD})}} \sim N^{2/d} \sqrt{\frac{m\mathcal{V}^2}{kR^2}}. \quad (52)$$

Systems where this is smaller than 1 can in principle be simulated with CD more efficiently than with MD, see Fig. 6.

$\frac{m\mathcal{V}^2}{kR^2}$  is the ratio between a typical kinetic energy per particle and the elastic energy cost to deform a particle substantially, i.e. on the scale of its radius. In most physical situations this factor should be small, because in general the kinetic energy does not suffice to deform collision partners substantially. In particular it is small for quasistatic systems of rigid particles. For such systems it is advantageous to take the limit of infinite rigidity and to use CD instead of MD, provided the particle number is not too large.

The factor  $N^{2/d} \propto N_I$  is the price for simulating perfectly rigid particles. For large systems with finite rigidity of the particles, MD costs less computing time than CD. However, if one is willing to use CD with incomplete force relaxation, i.e. with fixed  $N_I \ll N^{2/d}$ , the CD-algorithm leads to pseudo-elastic behaviour, analogous to soft particle MD-simulations [38].



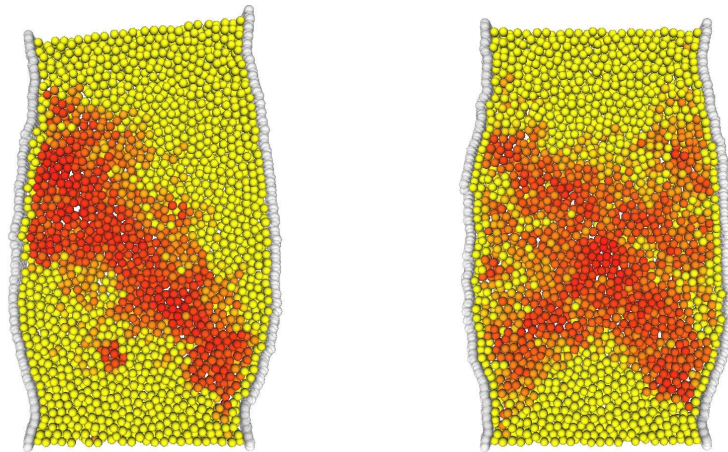


**Fig. 7:** *Localized shear zones in a three dimensional MD-simulation of the deformation of a cylindrical granular packing laterally confined by an elastic membrane. At the top and bottom there are rigid walls which move towards each other. The particle rotation speed is color coded. It is strong in regions with high shear rate. From [26].*

This involves sound propagation with finite speed and can be described by a damped wave equation. Then  $T_{\text{comp}}^{(\text{CD})} \sim T_{\text{comp}}^{(\text{MD})}$  even for large  $N$ .

## 4.2 Some recent applications

Contact Dynamics has been successfully applied to study the statistical properties of contact forces in a granular packing under load. A topic which is currently intensively studied is the non-uniqueness of realizations of force equilibrium in a dense frictional packing of rigid particles. Contact Dynamics is ideally suited to address this question [34].

Fig.7 on the other hand shows a Molecular Dynamics simulation of a large three dimensional system [26]. If the piston at the top is allowed to tilt one gets spontaneous symmetry breaking; if it remains parallel to the bottom, the shear zones maintain the cylindrical symmetry. I expect that a CD-simulation of this system would give the same result, but because of the large particle number ( $N = 27000$ ) would require more computing time if pseudo-elasticity were to be avoided. Indeed a comparative study [9] of a two dimensional packing similarly sheared as in Fig.7 gives *quantitative* agreement of the MD- and CD-results: Particle elasticity turned out to matter only, before the granular material yields.

## Acknowledgement

These lecture notes are based on the practical experience and algorithmic developments of many coworkers: I thank G. Bartels, L. Brendel, D. Kadau, F. Radjai and T. Unger for sharing their insights on CD, as well as L. Brendel, S. Dippel, S. Fazekas, M. Klocke, T. Scheffler, J. Schäfer, I. Severens, J. Török and J. Werth for sharing their insights on MD. Our simulation projects on granular matter are funded by DFG (within SFB 445 and grant WO 577/3), by Federal Mogul GmbH and by the German-Israeli-Foundation (795/2003). This work benefitted also from our earlier DFG-grant WO 577/1, BMBF-grant HUN 02/011, and the European Community network CHRX-CT93-0354.

## References

- [1] H. Hinrichsen, D. E. Wolf (eds.), *The Physics of Granular Media* (Wiley-VCH, Berlin, 2004)
- [2] H. J. Herrmann, J. P. Hovi, S. Luding (eds.), *Physics of Dry Granular Media* (Kluwer Academic Publishers, Dordrecht, 1998)
- [3] R. García-Rojo, H. J. Herrmann, S. McNamara (eds.), *Powders & Grains 05* (Balkema, Leiden, 2005)
- [4] D. Kadau, G. Bartels, L. Brendel, D. E. Wolf, *Phase Transitions* **76**, 315 (2003)
- [5] Th. Pöschel, Th. Schwager, *Computational Granular Dynamics* (Springer, Berlin, 2005)
- [6] R. A. Bagnold, *Proc. R. Soc. London A* **225**, 49 (1954)
- [7] D. E. Wolf, in: *Computational Physics*, eds. K. H. Hoffmann, M. Schreiber (Springer, Heidelberg, 1996) 64
- [8] G. Lois, A. Lemaître, J. M. Carlson, *Phys. Rev. E* **72**, 051303 (2005)
- [9] D. Kadau, D. Schwesig, J. Theuerkauf, D. E. Wolf, *Granular Matter*, DOI: 10.1007/s10035-005-0217-y (2005)
- [10] F. da Cruz, S. Emam, M. Prochnow, J.-N. Roux, F. Chevoir, *Phys. Rev. E* **72**, 021309 (2005)
- [11] D. E. Wolf, T. Scheffler, J. Schäfer, *Physica A* **274**, 171 (1999)
- [12] R. Brewster, G. S. Grest, J. W. Landry, A. J. Levine, *Phys. Rev. E* **72**, 061301 (2005)
- [13] D. E. Wolf, T. Unger, D. Kadau, L. Brendel, in: *Powders & Grains 05*, eds. R. García-Rojo, H. J. Herrmann, S. McNamara (Balkema, Leiden 2005) p.525
- [14] P. A. Cundall, O. D. L. Strack, *Géotechnique* **29**, 47 (1979)
- [15] S. Luding, in: *The Physics of Granular Media*, eds. H. Hinrichsen, D. E. Wolf (Wiley-VCH, Berlin, 2004) 299
- [16] W. H. Press, B. P. Flannery, S. A. Teukolsky, W. T. Vetterling, *Numerical Recipes* (Cambridge University Press, Cambridge, 1986)
- [17] G. Kuwabara, K. Kono, *Jap. J. Appl. Phys.* **26**, 1230 (1987)
- [18] K. L. Johnson, *Contact Mechanics* (Cambridge Univ. Press, Cambridge, 1989); L. D. Landau, E. M. Lifshitz, *Lehrbuch der Theoretischen Physik* Vol.VII: Elastizitätstheorie (Akademie-Verlag, Berlin, 1989)
- [19] N. V. Brilliantov, F. Spahn, J.-M. Hertzsch, Th. Pöschel, *Physica A* **231**, 417 (1996)
- [20] N. V. Brilliantov, Th. Pöschel, in: *The Physics of Granular Media*, eds. H. Hinrichsen, D. E. Wolf (Wiley-VCH, Berlin, 2004) 189

- [21] W. Goldsmith, *Impact* (Edward Arnold Publ., London, 1960)
- [22] F. G. Bridges, A. Hatzes, D. N. C. Lin, *Nature* **309**, 333 (1984)
- [23] R. Sondergaard, K. Chaney, C. E. Brennen, *J. Appl. Mech.* **57**, 694 (1990)
- [24] D. Elata, J. G. Berryman, *Mechanics of Materials* **24**, 229 (1996)
- [25] L. Brendel, S. Dippel, in: *Physics of Dry Granular Media*, eds. H. J. Herrmann, J. P. Hovi, S. Luding (Kluwer Academic Publishers, Dordrecht, 1998) 313
- [26] S. Fazekas, J. Török, J. Kertész, D. E. Wolf, in: *Powders & Grains 05*, eds. R. García-Rojo, H. J. Herrmann, S. McNamara (Balkema, Leiden 2005) p.223
- [27] S. Luding, E. Clément, A. Blumen, J. Rajchenbach, J. Duran, *Phys. Rev. E* **50**, 4113 (1994)
- [28] J. Schäfer, D. E. Wolf, *Phys. Rev. E* **51**, 6154 (1995)
- [29] L. Brendel, T. Unger, D. E. Wolf, in: *The Physics of Granular Media*, eds. H. Hinrichsen, D. E. Wolf (Wiley-VCH, Berlin, 2004) 325
- [30] P. Lötstedt, *SIAM J. Appl. Math.* **42**, 281 (1982)
- [31] M. Jean, *Comput. Methods Appl. Mech. Engrg.* **177**, 235 (1999)
- [32] J.J. Moreau, in: *Powders & Grains 93*, eds. C. Thornton (Balkema, Rotterdam, 1993) 227
- [33] F. Radjai, L. Brendel, S. Roux, *Phys. Rev. E* **54**, 861 (1996)
- [34] T. Unger, J. Kertész, D. E. Wolf, *Phys. Rev. Lett.* **94**, 178001 (2005)
- [35] Th. Schwager, Th. Pöschel, in: *System Dynamics of Long-Term Behaviour of Railway Vehicles, Track and Subgrade*, eds. K. Popp, W. Schiehlen (Springer, Berlin, 2002)
- [36] G. Bartels, *Die Kontakt-Dynamik-Methode*, Diplomarbeit, Univ. Duisburg (2001)
- [37] T. Unger, J. Kertész, in: *Modeling of Complex Systems*, eds. P. L. Garrido, J. Marro (AIP, New York, 2003) 116
- [38] T. Unger, L. Brendel, D. E. Wolf, J. Kertész, *Phys. Rev. E* **65**, 061305 (2002)